

# Dalton Transactions

Accepted Manuscript



This is an *Accepted Manuscript*, which has been through the Royal Society of Chemistry peer review process and has been accepted for publication.

*Accepted Manuscripts* are published online shortly after acceptance, before technical editing, formatting and proof reading. Using this free service, authors can make their results available to the community, in citable form, before we publish the edited article. We will replace this *Accepted Manuscript* with the edited and formatted *Advance Article* as soon as it is available.

You can find more information about *Accepted Manuscripts* in the [Information for Authors](#).

Please note that technical editing may introduce minor changes to the text and/or graphics, which may alter content. The journal's standard [Terms & Conditions](#) and the [Ethical guidelines](#) still apply. In no event shall the Royal Society of Chemistry be held responsible for any errors or omissions in this *Accepted Manuscript* or any consequences arising from the use of any information it contains.

Cite this: DOI: 10.1039/x0xx00000x

www.rsc.org/dalton

ARTICLE TYPE

# A series of divalent metal coordination polymers based on isomeric tetracarboxylic acids: Synthesis, structures and magnetic properties

Min-Le Han<sup>a,b</sup>, Ya-Ping Duan<sup>a</sup>, Dong-Sheng Li<sup>a\*</sup>, Guo-Wang Xu<sup>a</sup>, Ya-Pan Wu<sup>a</sup>, Jun Zhao<sup>a</sup><sup>5</sup> Received (in XXX, XXX) Xth XXXXXXXXX 20XX, Accepted Xth XXXXXXXXX 20XX

DOI: 10.1039/x0xx00000x

Five new coordination polymers, namely,  $[\text{Mn}(2,2'\text{-bipy})(\text{H}_2\text{O})_2(\text{H}_2\text{L}^1)]_n$  (**1**),  $\{[\text{Co}(\text{btb})(\text{H}_2\text{O})_2(\text{H}_2\text{L}^1)] \cdot 0.5\text{H}_2\text{O}\}_n$  (**2**),  $[\text{Co}(\text{bib})(\text{H}_2\text{O})_2(\text{H}_2\text{L}^1)]_n$  (**3**),  $[\text{Ni}_2(\text{bpm})(\text{H}_2\text{O})_3(\text{L}^2)]_n$  (**4**),  $\{[\text{Co}_2(\text{H}_2\text{O})_3(\text{OH})(\text{HL}^2)] \cdot \text{H}_2\text{O}\}_n$  (**5**), ( $\text{H}_4\text{L}^1 = 1,1':2',1''\text{-terphenyl-4,4',4'',5'-tetracarboxylic acid}$ ,  $\text{H}_4\text{L}^2 = 1,1':2',1''\text{-terphenyl-3,3'',4',5'-tetracarboxylic acid}$ ,  $2,2'\text{-bipy} = 2,2'\text{-bipyridine}$ ,  $\text{btb} = 1,4\text{-bis}(1,2,4\text{-triazol-1-yl})\text{butane}$ ,  $\text{bib} = 1,4\text{-bis}(\text{imidazol-1-yl})\text{butane}$ ,  $\text{bpm} = \text{bis}(4\text{-pyridyl})\text{amine}$ ), have been obtained under hydrothermal conditions. Complex **1** exhibits a 3D supramolecular framework based on 1D chain. Both complexes **2** and **3** are 3D supramolecular framework constructed by 1D zig-zag chain. Complex **4** features a 3D tetra-nodal (3,4,4,5)-connected architecture containing 1D  $\mu\text{-COO}$  bridged chains with  $(5^2.6^2.7.9)(5^2.6^4.7^3.8)_2(5^2.6)_2(6^3.7^2.9)$  topology. Complex **5** shows a 3D penta-nodal (3,4,4,6,6)-connected net containing 1D  $\mu\text{-OH}/\mu\text{-COO}$  bridged chains and mononuclear Co(II) nodes with a  $(4^2.6^3.8)(4^3)_2(4^4.6^2)_2(4^4.6^6.8^5)_2(4^4.6^7.8^4)$  topology. Variable-temperature magnetic susceptibility measurements reveals that complexes **2** and **3** show antiferromagnetic interactions between the adjacent Co(II) ions, whereas **4** is a ferromagnetic system.

## 20 Introduction

Studies of metal-organic frameworks (MOFs) or coordination polymers (CPs) is of considerable interest due to their fascinating network topologies and potential applications as functional materials.<sup>1-5</sup> Organic aromatic multicarboxylate, such as 1,2,4,5-benzenetetracarboxylate, as the mediators between the metal centers, can yield predetermined networks and have been widely utilized to construct coordination polymers.<sup>6,7</sup> As derivatives of 1,2,4,5-benzenetetracarboxylate, 1,1':2',1''-terphenyl-tetracarboxylic acid is a more flexible and bigger ligand. The four carboxyl groups of 1,1':2',1''-terphenyl-tetracarboxylic acid may be completely or partially deprotonated, inducing various coordination modes and allowing higher dimensionality structures, and can act as hydrogen bond acceptor/donor, depending upon the degree of deprotonation. On the other hand, three sets of carboxyl groups separated by phenyl group can form different dihedral angles through the rotation of C-C single bonds, thus it may ligate metal centres in different orientations. These characters may lead to various motifs with unique topologies.<sup>8</sup> Liu et al. prepared a novel 3D microporous complex  $[\text{Zn}_3(\text{HL}^1)(4,4'\text{-bipy})(\text{H}_2\text{O})_2]_n$  (MOF-COOH,  $\text{H}_4\text{L}^1 = 1,1':2',1''\text{-terphenyl-4,4',4'',5'-tetracarboxylic acid}$ ,  $4,4'\text{-bipy} = 4,4'\text{-bipyridine}$ ) containing uncoordinated carbonyl groups pointing to the pores. The MOF-COOH complex can effectively and selectively serve as an antenna for sensitizing the visible-emitting  $\text{Tb}^{3+}$  cation.<sup>9</sup> Meanwhile, the strategy of mixed-ligands assembly has been becoming an effective approach for the construction of

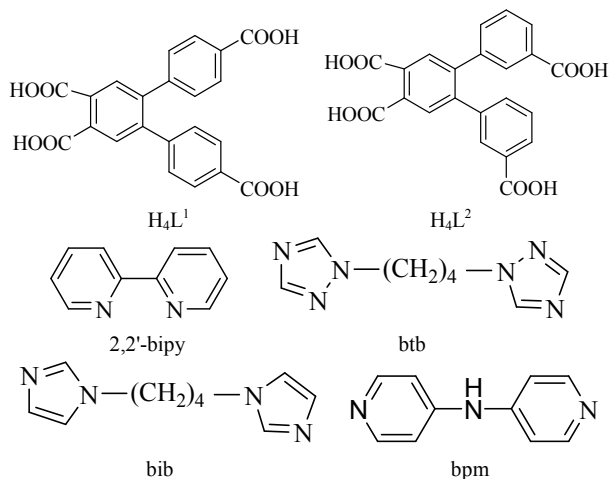
coordination frameworks with fascinating topologies and desirable properties<sup>1-4,5</sup>. Among them, the rigid/flexible N-donor ligands have been widely utilized in the construction of MOFs with various topologies.<sup>10,11</sup> According to previous studies, the rigid/flexible N-donor ligands, such as bis(pyridyl) or bis(imidazol-1-yl) or bis(1,2,4-triazol-1-yl) ligands have significant influence on the assembly systems of multicarboxylate ligands and metal centers.<sup>12-14</sup> In this work, we selected isomeric tetracarboxylic acid, 1,1':2',1''-terphenyl-4,4',4'',5'-tetracarboxylic acid ( $\text{H}_4\text{L}^1$ ) or 1,1':2',1''-terphenyl-3,3'',4',5'-tetracarboxylic acid ( $\text{H}_4\text{L}^2$ ) as a bridging ligand and reacted it with/without rigid/flexible N-donor ligand and Mn(II)/Co(II)/Ni(II) ions under hydrothermal conditions, which gave rise to five coordination polymers, namely  $[\text{Mn}(2,2'\text{-bipy})(\text{H}_2\text{O})_2(\text{H}_2\text{L}^1)]_n$  (**1**),  $\{[\text{Co}(\text{btb})(\text{H}_2\text{O})_2(\text{H}_2\text{L}^1)] \cdot 0.5\text{H}_2\text{O}\}_n$  (**2**),  $[\text{Co}(\text{bib})(\text{H}_2\text{O})_2(\text{H}_2\text{L}^1)]_n$  (**3**),  $[\text{Ni}_2(\text{bpm})(\text{H}_2\text{O})_3(\text{L}^2)]_n$  (**4**),  $\{[\text{Co}_2(\text{H}_2\text{O})_3(\text{OH})(\text{HL}^2)] \cdot \text{H}_2\text{O}\}_n$  (**5**). Herein, we report their syntheses, crystal structures, thermogravimetric analysis and magnetic properties.

## Experimental

### Materials and Physical Measurements

All solvents and reagents for synthesis were commercially purchased and used as received. Elemental analyses for carbon, hydrogen and nitrogen were performed on a Perkin-Elmer 2400 Series II analyzer. The infrared spectra ( $4000 \sim 400 \text{ cm}^{-1}$ ) were recorded as KBr pellets a FTIR Nexus spectrometer. Powder X-ray diffraction (PXRD) patterns for samples were taken on a Rigaku Ultima IV diffractometer (Cu  $K\alpha$  radiation,  $\lambda = 1.5406 \text{ \AA}$ ),

with a scan speed of 8 °/min and a step size of 0.02 ° in  $2\theta$ . The calculated PXRD patterns were simulated by using the single-crystal X-ray diffraction data. Thermogravimetric (TG) curves were recorded on a NETZSCH STA 449C microanalyzer in air atmosphere at a heating rate of 10 °C/min. Variable-temperature magnetic susceptibility measurements (2-300 K) were carried out on a Quantum Design PPMS60000 in a magnetic field of 1 KOe, and the diamagnetic corrections were evaluated by using Pascal's constants.



**Scheme 1** Structures of the  $H_4L^1$ ,  $H_4L^2$ , and N-donor ligands used in this work.

### Preparation of Complexes 1-5

#### [Mn(2,2'-bipy)(H<sub>2</sub>O)<sub>2</sub>(H<sub>2</sub>L<sup>1</sup>)<sub>n</sub>] (1)

A mixture of  $H_4L^1$  (0.1 mmol, 40.6 mg), 2,2'-bipy (0.10 mmol, 15.6 mg), Mn(OAc)<sub>2</sub>·4H<sub>2</sub>O (0.1 mmol, 22.2 mg), KOH (0.2 mmol, 11.2 mg) and H<sub>2</sub>O (10 mL) was placed in a Teflon-lined stainless steel vessel (25 mL), heated to 160 °C for 3 days, and then cooled to room temperature over 24 h. Pink brism crystals of **1** were obtained. Yield: 27.4 mg, 42% (based on Mn). Elemental analysis (%): calcd for C<sub>32</sub>H<sub>24</sub>MnN<sub>2</sub>O<sub>10</sub> ( $M_r = 651.47$ ): C 59.00, H 3.71, N 4.30; found: C 59.08, H 3.66, N 4.23. IR (cm<sup>-1</sup>): 3434(m), 1716(m), 1687(m), 1599(s), 1551(s), 1438(s), 1355(s), 748(s).

#### {[Co(btb)(H<sub>2</sub>O)<sub>2</sub>(H<sub>2</sub>L<sup>1</sup>)]·0.5H<sub>2</sub>O}<sub>n</sub> (2)

**2** was prepared by the similar method as that described for **1**, except that bipy was replaced by btb (0.1 mmol, 19.3 mg) and Mn(OAc)<sub>2</sub>·4H<sub>2</sub>O was replaced by Co(OAc)<sub>2</sub>·4H<sub>2</sub>O (0.1 mmol, 22.5 mg). Red brism crystals of **2** were obtained. Yield: 24.5 mg, 40% (based on Co). Elemental analysis (%): calcd for C<sub>26</sub>H<sub>23</sub>CoN<sub>3</sub>O<sub>10.5</sub> ( $M_r = 604.40$ ): C 51.67, H 3.84, N 6.95; found: C 50.85, H 3.98, N 6.78. IR (cm<sup>-1</sup>): 3490(m), 1683(s), 1541(m), 1384(m), 1281(s), 1186(m), 1134(m), 794(m).

#### [Co(bib)(H<sub>2</sub>O)<sub>2</sub>(H<sub>2</sub>L<sup>1</sup>)<sub>n</sub>] (3)

**3** was prepared by the similar method as that described for **2**, except that btb was replaced by bib (0.1 mmol, 19.0 mg). Red brism crystals of **3** were obtained. Yield: 24.9 mg, 42% (based on Co). Elemental analysis (%): calcd for C<sub>27</sub>H<sub>23</sub>CoN<sub>2</sub>O<sub>10</sub> ( $M_r = 594.40$ ): C 54.56, H 3.90, N 4.71; found: C 54.63, H 3.95, N 4.78. IR (cm<sup>-1</sup>): 3489(m), 1680(s), 1544(m), 1384(m), 1285(s), 1186(m), 1130(m), 790(m).

#### [Ni<sub>2</sub>(bpm)(H<sub>2</sub>O)<sub>3</sub>(L<sup>2</sup>)<sub>n</sub>] (4)

A mixture of  $H_4L^2$  (0.1 mmol, 40.6 mg), bpm (0.10 mmol, 17.1 mg), Ni(OAc)<sub>2</sub>·4H<sub>2</sub>O (0.1 mmol, 24.8 mg), KOH (0.4 mmol, 22.4 mg) and H<sub>2</sub>O (10 mL) was placed in a Teflon-lined stainless steel vessel (25 mL), heated to 160 °C for 3 days, and then cooled to room temperature over 24 h. Green brism crystals of **4** were obtained. Yield: 13.0 mg, 35% (based on Ni). Elemental analysis (%): calcd for C<sub>32</sub>H<sub>25</sub>N<sub>3</sub>Ni<sub>2</sub>O<sub>11</sub> ( $M_r = 744.97$ ): C 34.19, H 3.97, N 9.20; found: C 34.15, H 3.94, N 9.25. IR (cm<sup>-1</sup>): 3470(m), 1601(s), 1547(s), 1520(s), 1410(s), 1389(s), 751(s).

#### {[Co<sub>2</sub>(H<sub>2</sub>O)<sub>3</sub>(OH)(HL<sup>2</sup>)]·H<sub>2</sub>O}<sub>n</sub> (5)

A mixture of  $H_4L^2$  (0.1 mmol, 40.6 mg), Co(OAc)<sub>2</sub>·4H<sub>2</sub>O (0.1 mmol, 24.8 mg), KOH (0.4 mmol, 22.4 mg) and H<sub>2</sub>O (10 mL) was placed in a Teflon-lined stainless steel vessel (25 mL), heated to 160 °C for 3 days, and then cooled to room temperature over 24 h. Red brism crystals of **5** were obtained. Yield: 1.2 mg, 4% (based on Co). Elemental analysis (%): calcd for C<sub>22</sub>H<sub>20</sub>Co<sub>2</sub>O<sub>13</sub> ( $M_r = 610.24$ ): C 43.30, H 3.30; found: C 43.35, H 3.34. IR (cm<sup>-1</sup>): 3470(m), 1605(s), 1544(s), 1522(s), 1413(s), 1390(s), 753(s).

### X-Ray Crystallography

Single crystal X-ray diffraction analyses of **1–5** were carried out on a Rigaku XtaLAB mini diffractometer with graphite monochromated MoK $\alpha$  radiation ( $\lambda = 0.71073$  Å) at room temperature. The collected data were reduced using the program CrystalClear<sup>15</sup> and an empirical absorption correction was applied. All structures were solved by direct methods and refined based on  $F^2$  by the full-matrix least-squares methods using SHELXTL.<sup>16</sup> All non-H atoms were refined anisotropically. The H atoms were assigned with common isotropic displacement factors and included in the final refinement with restraints. The crystallographic data are listed in Table 1. Selected bond lengths and angles for **1–5** are listed in Table S1, shown in Electronic Supplementary Information.

## Results and Discussion

### Description of Crystal Structures

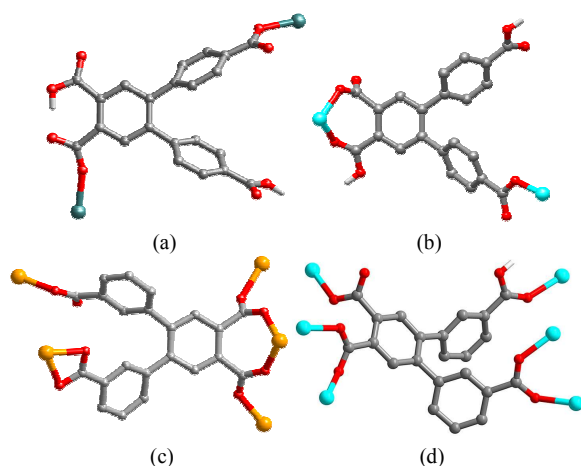
[Mn(2,2'-bipy)(H<sub>2</sub>O)<sub>2</sub>(H<sub>2</sub>L<sup>1</sup>)<sub>n</sub>] (**1**). There are one Mn (II) ion, one 2,2'-bipy, two coordinated water molecule and one H<sub>2</sub>L<sup>1</sup> ligand in the asymmetric unit of **1**. As shown in Fig. 1a, Mn1 center takes a distorted octahedron geometry, in which two oxygen atoms (Mn–O = 2.1047(18) and 2.1206(17) Å) from two H<sub>2</sub>L<sup>1</sup> ligands and two nitrogen atoms (Mn–N = 2.283(2) and 2.292(2) Å) from 2,2'-bipy form the equatorial plane and the apical positions are occupied by two water molecules (Mn–O = 2.204(2) and 2.2120(17) Å) with the O9–Mn1–O10 angle of 176.64(7) °. In **1**, 4,4'-carboxylic group of H<sub>2</sub>L<sup>1</sup> is undeprotonated and free of coordination. The other two carboxylate groups of H<sub>2</sub>L<sup>1</sup> ligand display ( $\kappa^1$ )-( $\kappa^1$ )- $\mu_2$  coordination fashion to link two Mn (II) atoms (Scheme 2a). The adjacent Mn (II) atoms are linked by  $\mu_2$ -H<sub>2</sub>L<sup>1</sup> to generate a 1D chain (Fig. 1b). Such 1D chains are further connected by hydrogen bonding between two undeprotonated carboxylic groups from different H<sub>2</sub>L<sup>1</sup> ( $d(O\cdots O) = 2.58$  Å,  $\angle(OHO) = 169.5$  °) to generate a 2D network. And the 2D networks are further linked by hydrogen bonding between the coordinated-water molecules and undeprotonated carboxylic groups ( $d(O\cdots O) = 2.88$  Å,  $\angle(OHO) = 168.6$  °), to form a 3D supramolecular architecture (Fig. 1c, Table S2, ESI).

{[Co(btb)(H<sub>2</sub>O)<sub>2</sub>(H<sub>2</sub>L<sup>1</sup>)]·0.5H<sub>2</sub>O}<sub>n</sub> (**2**) and

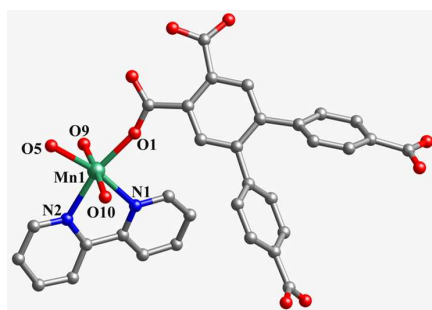
**Table 1.** Crystal and Structure Refinement Data for Complexes 1–5.

	1	2	3	4	5
Empirical formula	C <sub>32</sub> H <sub>24</sub> MnN <sub>2</sub> O <sub>10</sub>	C <sub>26</sub> H <sub>23</sub> CoN <sub>3</sub> O <sub>10.5</sub>	C <sub>27</sub> H <sub>23</sub> CoN <sub>2</sub> O <sub>10</sub>	C <sub>32</sub> H <sub>25</sub> N <sub>3</sub> Ni <sub>2</sub> O <sub>11</sub>	C <sub>22</sub> H <sub>20</sub> Co <sub>2</sub> O <sub>13</sub>
Formula weight	651.47	604.40	594.40	744.97	610.24
Temperature/K	296(2)	296(2)	296(2)	296(2)	296(2)
Crystal system	Triclinic	Monoclinic	Monoclinic	Monoclinic	Monoclinic
Space group	<i>P</i> $\bar{1}$	<i>C2/c</i>	<i>C2/c</i>	<i>P2<sub>1</sub>/c</i>	<i>P2<sub>1</sub>/c</i>
<i>a</i> /Å	10.454(5)	28.966(4)	28.550(2)	15.896(7)	14.444(8)
<i>b</i> /Å	10.739(5)	7.6922(7)	7.7222(7)	7.823(3)	6.526(4)
<i>c</i> /Å	13.686(7)	24.702(3)	24.645(2)	23.210(10)	23.959(13)
$\alpha$ /°	99.384(6)	90.00	90.00	90.00	90.00
$\beta$ /°	99.642(6)	107.507(6)	106.196(19)	92.895(7)	97.852(7)
$\gamma$ /°	94.786(6)	90.00	90.00	90.00	90.00
<i>V</i> /Å <sup>3</sup>	1484.8(12)	5249.0(11)	5217.8(7)	2883(2)	2237(2)
<i>Z</i>	2	8	8	4	4
<i>D<sub>c</sub></i> /g cm <sup>-3</sup>	1.457	1.530	1.513	1.717	1.812
$\mu$ /mm <sup>-1</sup>	0.507	0.720	0.720	1.379	1.557
<i>F</i> (000)	670	2488	2448	1528	1240
2 $\theta$ Range/°	1.53 – 27.52	1.73 – 25.50	2.57 – 27.54	1.76 – 27.55	2.85 – 27.56
Reflns. collected	15990	23051	26592	29630	23079
Independent reflns.	6797	4879	5976	6618	5179
<i>R<sub>int</sub></i>	0.0500	0.0854	0.0920	0.0722	0.0675
Data/restraints/parameters	6797/8/418	4879/0/370	5976/6/363	6618/9/442	5179/0/337
GOOF	1.080	1.074	1.067	1.066	1.030
<i>R</i> <sub>1</sub> <sup>a</sup>	0.0473	0.0543	0.0496	0.0446	0.0387
<i>wR</i> <sub>2</sub> <sup>b</sup> [ <i>I</i> > 2 $\sigma$ ( <i>I</i> )]	0.1263	0.1416	0.1087	0.1273	0.1011
<i>R</i> <sub>1</sub> (all data)	0.0637	0.0769	0.0685	0.0504	0.0497
<i>wR</i> <sub>2</sub> (all data)	0.1435	0.1623	0.1202	0.1325	0.1080
$\Delta\rho_{max}$ and $\Delta\rho_{min}$ (e.Å <sup>-3</sup> )	0.340, -0.442	0.551, -0.599	0.298, -0.538	1.143, -1.120	0.660, -0.576

<sup>a</sup>  $R_1 = \Sigma(|F_o| - |F_c|) / \Sigma |F_o|$ ; <sup>b</sup>  $wR_2 = \{\Sigma[w(|F_o|^2 - |F_c|^2)^2] / \Sigma[w(|F_o|^2)^2]\}^{1/2}$ .



**Scheme 2** Coordination modes of H<sub>2</sub>L<sup>1</sup> and L<sup>2</sup> ligands in this work (a for 1, b for 2 and 3, c for 4 and d for 5).



(a)

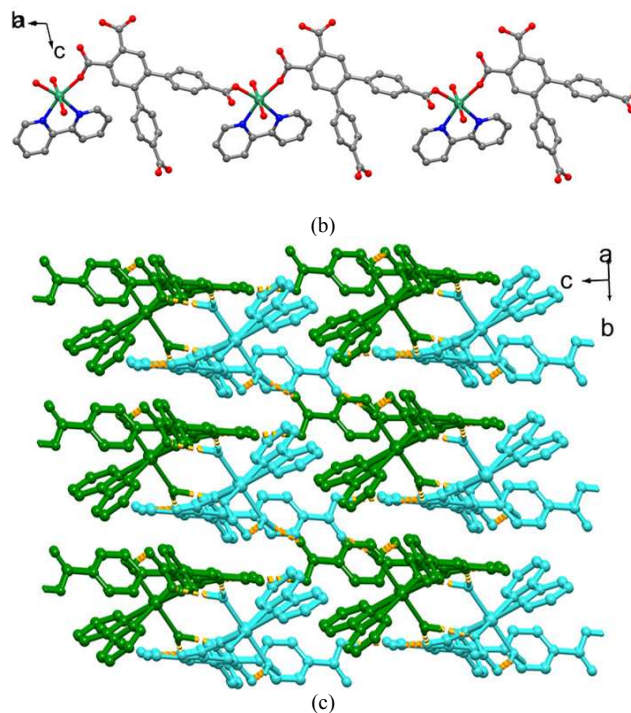


**Fig. 1** (a) Coordination environments of Mn(II) ion in 1. (b) View of the 1D chain. (c) View of 3D supramolecular structure. Hydrogen bonds are represented as light orange dash line.

[Co(bib)(H<sub>2</sub>O)<sub>2</sub>(H<sub>2</sub>L<sup>1</sup>)]<sub>n</sub> (**3**). Complexes **2** and **3** crystallize in the same monoclinic space group *C2/c*, and X-ray crystallography reveals that they have the same skeleton structure except half free

water molecule. Thus, only the structure of **2** is described in detail here. Complex **2** comprises one Co(II) atom, one btb ligand, one H<sub>2</sub>L<sup>1</sup> ligand, two coordinated water molecule and one free water molecule. As depicted in Fig. 2a, Co1 surrounded by one nitrogen atom from one btb and three carboxylate oxygen atoms from two different H<sub>2</sub>L<sup>1</sup> and two coordinated water. The Co-N bond length is 2.094(3) Å and Co-O ones are in the range of 2.059(3)-2.205(3) Å. 4",5'-Carboxylic group of H<sub>2</sub>L<sup>1</sup> is undeprotonated and 4"-carboxylic group is free of coordination. The other three carboxylate groups of H<sub>2</sub>L<sup>1</sup> ligand display (κ<sup>1</sup>)-(κ<sup>1</sup>)-(κ<sup>1</sup>)-μ<sub>2</sub> binding fashion to link two Co(II) atoms (Scheme 2b). Thus, the Co(II) atoms are bridged by H<sub>2</sub>L<sup>1</sup> ligands and μ<sub>2</sub>-btb to form a 1D zig-zag chain (Fig. 2b).

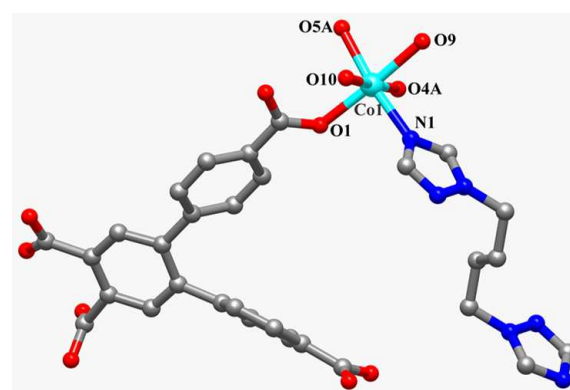
Two kinds of hydrogen bonding are present: (a) hydrogen bonding between undeprotonated carboxylic group and carboxylate O atom of H<sub>2</sub>L<sup>1</sup> ligands with O...O distances of 2.50 and 2.57 Å, respectively; (b) hydrogen bonding between coordinated water molecules and carboxylate O atoms of H<sub>2</sub>L<sup>1</sup> ligands with O...O distances of 2.65-3.13 Å. For complex **2**, the free water molecules are located by hydrogen bonds among btb, and carboxylate O atoms of H<sub>2</sub>L<sup>1</sup> ligands. These hydrogen bonding interactions not only brings further stability for the structure but also link the 1D zig-zag chains to form a 3D supramolecular architecture (Fig. 2c, Table S2, ESI)

[Ni<sub>2</sub>(bpm)(H<sub>2</sub>O)<sub>3</sub>(L<sup>2</sup>)]<sub>n</sub> (**4**). There are three crystallographic independent Ni(II) atoms, each taking a distorted octahedral coordination sphere (Fig. 3a). Ni1 is six-coordinated by two oxygen atoms from two L<sup>2</sup> ligands (Ni-O = 2.041(2) Å), two coordinated water molecules (Ni-O = 2.110(2) Å) and two nitrogen atom from two bpm (Ni-N = 2.094(2) Å). The Ni2 center is coordinated by four oxygen atoms from two L<sup>2</sup> ligands (Ni-O = 2.032(2)-2.185(2) Å), one coordinated water (Ni-O = 2.137(2) Å) and one nitrogen atom from two bpm (Ni-N = 2.032(2) Å). The Ni3 is coordinated by two aqua ligands and four oxygen atoms from four L<sup>2</sup> ligands. The Ni-O bond lengths are in the range of 2.041(2)- 2.090(2) Å. Four carboxylate groups of L<sup>2</sup> ligand adopt the (κ<sup>1</sup>-κ<sup>1</sup>)-(κ<sup>1</sup>-κ<sup>1</sup>)-(κ<sup>2</sup>)-(κ<sup>1</sup>)-μ<sub>5</sub> coordination fashion to bridge one Ni1, two Ni2 and two Ni3 (Scheme 1c). The Ni1, Ni2 and Ni3 atoms are bridged by two carboxylate groups in *syn,anti* fashion to form a 1D chain with the Ni...Ni distances of 5.24 and 5.30 Å, respectively. (Fig. 3b). Such 1D chains are further interlinked by L<sup>2</sup> and bpm ligands to form a 3D network (see Fig. 3c)

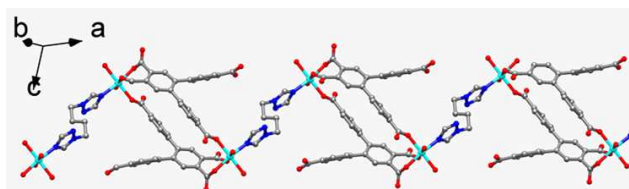
Analysis of the network topology of **4** reveals that Ni2 center acts as a 3-connected node. Ni1 and Ni3 act as 4-connected nodes. And the L<sup>2</sup> ligands serve as the 5-connected nodes. According to the simplification principle, the 3D structure of **4** is a (3,4,4,5)-connected net with stoichiometry (3-c)<sub>2</sub>(4-c)(4-c)(5-c)<sub>2</sub> (Fig. 3d). Topological analysis of the net indicates a (5<sup>2</sup>.6<sup>2</sup>.7.9)(5<sup>2</sup>.6<sup>4</sup>.7<sup>3</sup>.8)<sub>2</sub> (5<sup>2</sup>.6)<sub>2</sub>(6<sup>3</sup>.7<sup>2</sup>.9) topology.

{[Co<sub>2</sub>(H<sub>2</sub>O)<sub>3</sub>(OH)(HL<sup>2</sup>)]·H<sub>2</sub>O}<sub>n</sub> (**5**). The crystal structure of **5** shows a 3D network with 1D μ-OH/μ-COO bridged chains and mononuclear Co(II) nodes bridging by the HL<sup>2</sup> ligands. There are three crystallographic independent Co(II) ions, each taking a distorted octahedral coordination sphere (Fig. 4a). Co1 ion is six-coordinated by four O atoms from four HL<sup>2</sup> ligands and two water molecules. The Co-O bond lengths are in the range of

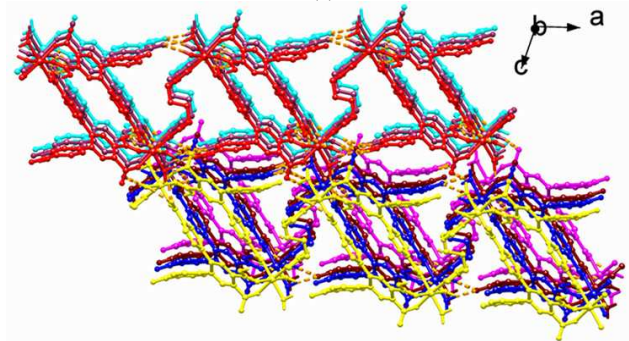
2.069(2)- 2.120(2) Å. Co2 ions are six-coordinated by two μ<sub>3</sub>-OH (Co-O = 2.0853(18) Å) and four oxygen atoms from four HL<sup>2</sup> ligands (Co-O = 2.0958(19) and 2.110(2) Å). Co3 is coordinated by two carboxylate atoms (Co-O = 2.0821(19) and 2.0974(18) Å), two water molecules (Co-O = 2.160(2) and 2.1678(19) Å) and two μ<sub>3</sub>-OH (Co-O = 2.0761(17) and 2.0873(18) Å). In **5**, 3-carboxylic group of HL<sup>1</sup> is undeprotonated and HL<sup>2</sup> ligand links six Co(II) in the (κ<sup>1</sup>-κ<sup>1</sup>)-(κ<sup>1</sup>-κ<sup>1</sup>)-(κ<sup>1</sup>)-(κ<sup>1</sup>)-μ<sub>6</sub> coordination fashion. The Co2 and Co3 ions are bridged by the carboxylate groups in (κ<sup>1</sup>-κ<sup>1</sup>)-(κ<sup>1</sup>-κ<sup>1</sup>) modes and μ<sub>3</sub>-OH to form a 1D chain. Such 1D chains are further connected by the HL<sup>2</sup> ligands *via* [Co(H<sub>2</sub>O)<sub>2</sub>O<sub>4</sub>] units along different directions to form a 3D network (Fig. 4b). From the view of topology, μ<sub>3</sub>-OH can be considered as the 3-connected node. Co1 and Co3 can be considered as the 4-connected node, while Co2 and HL<sup>2</sup> ligand serve as a 6-connected node. According to the simplification principle, the 3D structure of **5** is a (3,4,4,6,6)-connected net with stoichiometry (3-c)<sub>2</sub>(4-c)(4-c)(6-c)<sub>2</sub>(6-c) (Fig. 4c). Topological analysis of the net indicates a (4<sup>2</sup>.6<sup>3</sup>.8)(4<sup>3</sup>)<sub>2</sub>(4<sup>4</sup>.6<sup>2</sup>)<sub>2</sub>(4<sup>4</sup>.6<sup>6</sup>.8<sup>5</sup>)<sub>2</sub>(4<sup>4</sup>.6<sup>7</sup>.8<sup>4</sup>) topology.



(a)

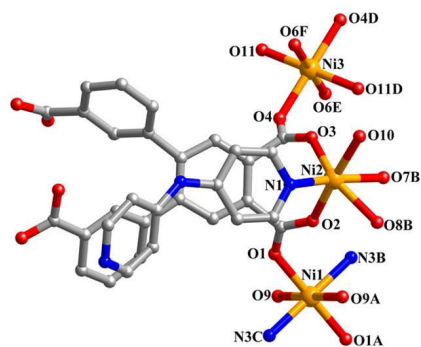


(b)

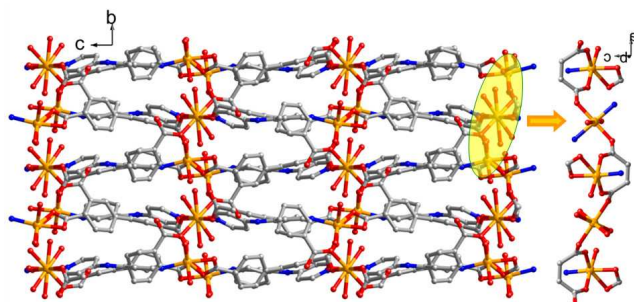


(c)

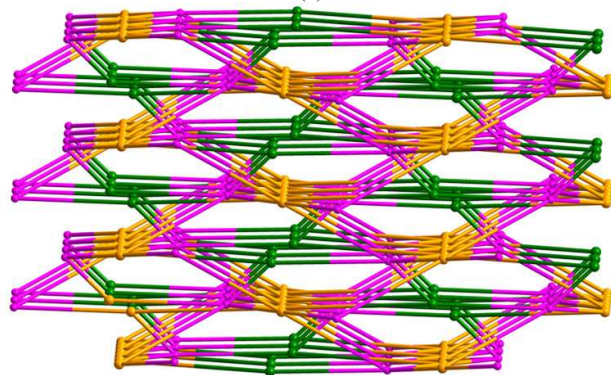
**Fig. 2** (a) Coordination environments of Co(II) ion in **2** (symmetry codes: 85 A: - x, - y + 1, - z + 1). (b) View of the 1D chain of **2**. (c) View of 3D supramolecular structure. Free water molecules are omitted for clarity. Hydrogen bonds are represented as light orange dash line.



(a)



(b)



(c)

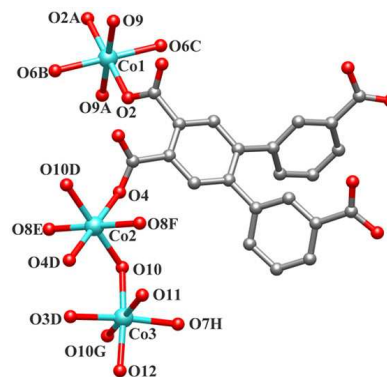
**Fig. 3** (a) Coordination environments of Ni(II) ions in **4** (symmetry codes: A:  $-x + 1, -y + 2, -z + 1$ ; B:  $x, -y + 3/2, z + 1/2$ ; C:  $-x + 1, y + 1/2, -z + 1/2$ ; D:  $-x, -y + 2, -z + 1$ ; E:  $x, -y + 5/2, z + 1/2$ ; F:  $-x, y - 1/2, -z + 1/2$ ). (b) View of the 3-D architecture of **4**. (c) Schematic representation of the (3, 4, 4, 5)-connected net with  $(5^2.6^2.7.9)(5^2.6^4.7^3.8)_2(5^2.6)_2(6^3.7^2.9)$  topology in **4**. (green: Ni2 nodes; gold: Ni1 and Ni3 nodes; pink: L2 ligand nodes)

### 15 Synthetic Chemistry and Structural Diversity

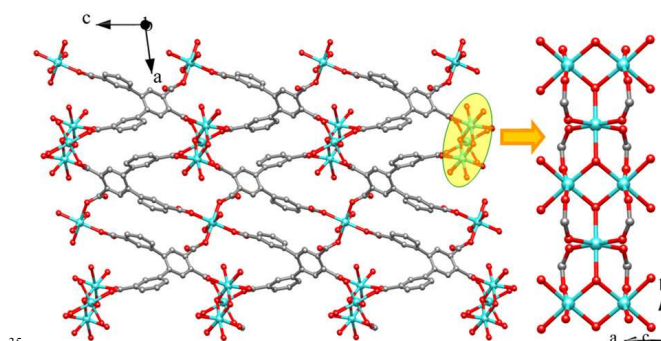
$H_4L^1$  and  $H_4L^2$  are a pair of isomeric tetracarboxylic acid, which differ in the position of two carboxylic groups. In the present study, five new complexes were successfully synthesized.

Parallel experiments show that the pH values of the reaction system are crucial for formation of compounds **1–5**. Complexes **1–3** could only be obtained in the special pH values of  $\sim 4$ , while complexes **4** and **5** could only be obtained in the special pH values of  $\sim 7$ . When the pH value is lower or higher than that special value, the expected crystals could not be obtained. We assume that several factors together with the co-existence of N-donor ligands directed the final structures, such as the reaction pH, the thermodynamic and kinetic equilibrium, and so on.<sup>17</sup>

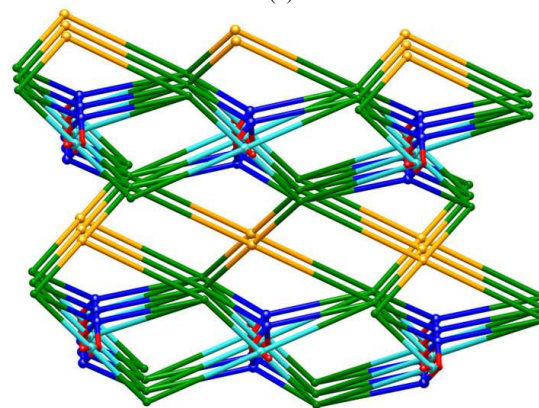
As we all know, coordination modes of multicarboxylate ligand play a vital role on the structures of final products. According to previous references, The four carboxyl groups of  $H_4L^1$  may be completely or partially deprotonated, inducing various



(a)



(b)



(c)

**Fig. 4** (a) Coordination environments of Co(II) ions in **5** (symmetry codes: A:  $-x + 2, -y - 1, -z + 1$ ; B:  $x, -y - 1/2, z + 1/2$ ; C:  $-x + 2, y - 1/2, -z + 1/2$ ; D:  $-x + 1, -y, -z + 1$ ; E:  $x, -y + 1/2, z + 1/2$ ; F:  $-x + 1, y - 1/2, -z + 1/2$ ; G:  $-x + 1, -y + 1, -z + 1$ ; H:  $-x + 1, y + 1/2, -z + 1/2$ ). (b) View of the 2D layer of **5**. (c) Schematic representation of the (3, 4, 4, 6, 6)-connected net of **5** with a  $(4^2.6^3.8)(4^3)_2(4^4.6^2)_2(4^4.6^6.8^5)_2(4_4.6^7.8^4)$  topology. (red: O nodes; light orange: Co1 nodes; aqua: Co2 nodes; blue: Co3 nodes; green: L2 ligand nodes)

modes. For complexes **1–3**, two carboxylic groups of  $H_4L^1$  is undeprotonated and free of coordination for **1** while only one undeprotonated carboxylic groups free of coordination for **2** and **3**. In **1**, the other two carboxylate groups of  $H_2L^1$  ligand display  $(\kappa^1)-(\kappa^1)-\mu_2$  coordination fashion to link two Mn (II) atoms

(Scheme 2a). Thus **1** shows a 1D chain. In **2** and **3**, three carboxylate groups of  $H_2L^1$  ligand display  $(\kappa^1)-(\kappa^1)-(\kappa^1)-\mu_2$  binding fashion to link two Co(II) atoms (Scheme 2b). So **2** and **3** display 1D zig-zag chains.

For  $\{[Co_3(HL^1)_2(bpe)_3(H_2O)_2] \cdot 6H_2O\}_n$  (**6**,  $bpe = 1,2$ -bi(4-pyridyl)ethene),<sup>8a</sup> the  $H_4L^1$  is partially deprotonated as  $HL^1$  and the ligand displays  $(\kappa^1-\kappa^1)-(\kappa^2-\mu_2)-\mu_4$  binding fashions. In **6**, three Co(II) atoms are held together by carboxylate groups to form a trinuclear unit, and the trinuclear units are expanded by  $HL^1$  and  $bpe$  ligands to form a 2D double-deck network. For  $\{[Co_2(H_2O)_5(H_2L^1)] \cdot 10H_2O\}_n$  (**7**),<sup>8a</sup> two carboxylate groups of  $H_4L^1$  are deprotonated. In **7**,  $H_2L^1$  ligand shows  $(\kappa^1-\kappa^1)-(\kappa^1)-\mu_3$  coordinated modes. Thus two adjacent Co(II) are combined by carboxylic groups to form a  $Co_2$  unit. The units are bridged by  $H_2L^1$  ligands to generate a grid chain. While for  $\{[Cd_2(2,2'$ -bipy)( $H_2O)_2(L^1)] \cdot H_2O\}_n$  (**8**),<sup>8b</sup>  $[Co_2(L^1)(pyridine)(H_2O)_3]_n$  (**9**),<sup>8a</sup> and  $\{[Co_2(L^1)(4,4'$ -bipy) $_{1.5}(H_2O)] \cdot H_2O\}_n$  (**10**,  $4,4'$ -bipyridine),<sup>8a</sup> the four carboxylate groups of  $H_4L^1$  are completely deprotonated. In **8**, **9** and **10**, four carboxylate groups display  $(\kappa^1)-(\kappa^1-\mu_2)-(\kappa^2-\mu_2)-(\kappa^1-\mu_2)-\mu_6$ ,  $(\kappa^1-\kappa^1)-(\kappa^1)-(\kappa^1-\kappa^1)-(\kappa^1-\kappa^1)-\mu_6$ , and  $(\kappa^1-\kappa^1)-(\kappa^1-\kappa^1)-(\kappa^2)-(\kappa^1)-\mu_5$ , binding fashions, respectively. In **6**, Four Cd(II) centers are linked by carboxylate groups, affording a  $Cd_4$  cluster. Thus complex **8** is a 3D porous structure building on  $Cd_4$  clusters SBUs. In **9**, Co(II) centers are connected by the carboxylate groups and  $\mu_2$ -aqua molecules to form a 1D chain. Such 1D chains are further connected by the  $L^1$  ligands to form a 2D double-decker layer. In **10**, the  $Co_2$  and  $Co_3$  atoms are bridged by the carboxylate groups to form a 1D wavelike chain. Such 1D chains are further connected by the  $L^1$  and  $4,4'$ -bipy ligands via  $[Co_1NO_3]_n$  units to form a 3D network.

For complex **4**,  $L^2$  ligand adopts  $(\kappa^1-\kappa^1)-(\kappa^1-\kappa^1)-(\kappa^2)-(\kappa^1)-\mu_5$  coordination fashion to coordinated five Ni(II) ions (Scheme 2c). So **4** has a tetranodal (3,4,4,5)-connected net with a  $(5^2.6^2.7.9)(5^2.6^4.7^3.8)_2(5^2.6)_2(6^3.7^2.9)$  topology. Although the coordination modes of multicarboxylate ligand in **4** are similar to those in **10**. **4** has (3,4,4,5)-connected 3D net with a  $(5^2.6^2.7.9)(5^2.6^4.7^3.8)_2(5^2.6)_2(6^3.7^2.9)$  topology, while **10** exhibits (4,4,4,5)-connected 3D architecture with a  $(4^2.6.8^2.10)_2(4^2.6^3.8^5)_2(6^2.8^3.12)_2$  topology. In **4**, three crystallographic independent Ni(II) atoms are all six-coordinated with distorted octahedral coordination sphere, while in **10**,  $Co_1$  is four-coordinated with a distorted tetrahedron and  $Co_2$  and  $Co_3$  take on a distorted octagonal configuration. This may be due to they have different N-donor ligands and different dispositions of the carboxylate groups of multicarboxylate ligands. In **5**, the  $HL^2$  ligand links six Co(II) in the  $(\kappa^1-\kappa^1)-(\kappa^1-\kappa^1)-(\kappa^1)-(\kappa^1)-\mu_6$  coordination fashion. And **5** possesses a penta-nodal (3,4,4,6,6)-connected net with a  $(4^2.6^3.8)(4^3)_2(4^4.6^2)_2(4^4.6^6.8^5)_2(4^4.6^7.8^4)$  topology.

### PXRD and Thermal Analysis

In order to check the phase purity of complexes **1–4**, the powder X-ray diffraction (PXRD) patterns of these complexes were checked at room temperature. As shown in Fig. S1 (ESI), the peak positions of the simulated and experimental PXRD patterns are in agreement with each other, demonstrating the good phase purity of the complexes.

Complexes **1–4** are air stable, insoluble in common organic solvents, and can retain their crystalline integrity at ambient

condition for a long time. The thermal behaviors of **1–4** were studied by thermogravimetric analysis (TGA). The experiments were performed on samples consisting of numerous single crystals under  $N_2$  atmosphere with a heating rate of  $10\text{ }^\circ\text{C min}^{-1}$ , as shown in Fig. S2 (ESI). For complex **1**, the first weight loss of 5.4% (calcd. 5.5%) was observed from 135 to 165  $^\circ\text{C}$  corresponding to the loss of free water molecules. Then pyrolysis of the sample occurred from  $\sim 270$  to 650  $^\circ\text{C}$ . The removal of water molecules can be observed for **2** with the weight loss of 7.9% (calc. 7.4%) from 75 to 200  $^\circ\text{C}$ . Then pyrolysis of the sample occurred from  $\sim 200$  to 615  $^\circ\text{C}$ . The final residue of 10.5% is close to the calculated 12.4% based on  $CoO$ . Complex **3** exhibited no mass loss until  $\sim 170\text{ }^\circ\text{C}$ , at which point a series of mass losses ensued. Complex **4** loses the lattice water molecules at 230–295  $^\circ\text{C}$  (calc. 7.3% and exp. 8.2%). The final mass remnant of 19.9% at 580  $^\circ\text{C}$  likely represents the deposition of NiO (20.1% calcd).

### Magnetic Properties of 2-4

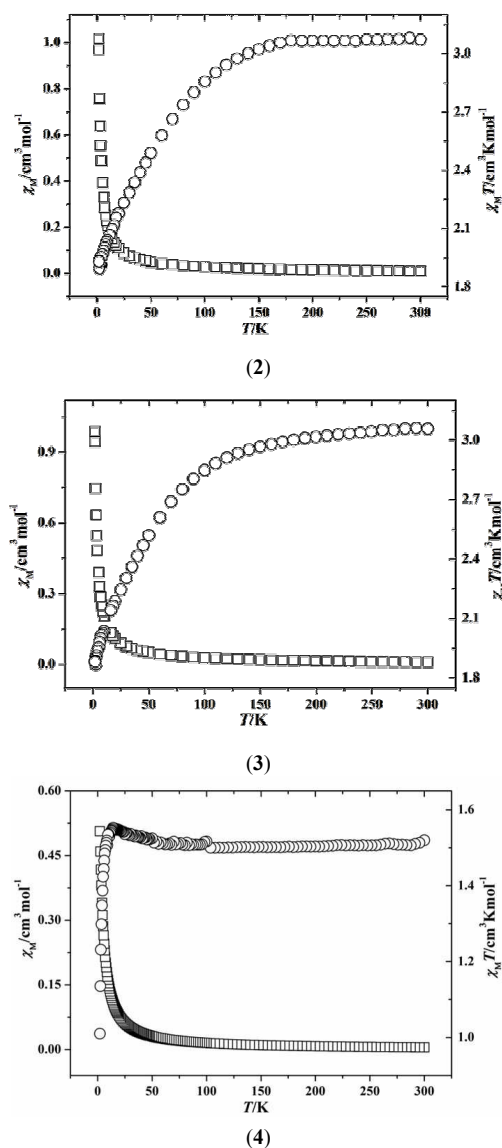


Fig. 5 Temperature dependence of  $\chi_M T$  and  $\chi_M$  versus  $T$  for **2–4**. Circle symbols represent  $\chi_M T$  and square symbols represent  $\chi_M$ .

The magnetic susceptibilities,  $\chi_M$ , of **2-4** were measured in the temperature range of 2-300 K at 1,000 Oe (Fig. 5). For complex **2** and **3**, the experimental  $\chi_M T$  value at room temperature is 3.07 and 3.06  $\text{cm}^3 \cdot \text{mol}^{-1} \cdot \text{K}$ , respectively, which is larger than the spin-only value (1.875  $\text{cm}^3 \cdot \text{mol}^{-1} \cdot \text{K}$  with  $g = 2.0$ ) expected for a magnetically isolated Co(II) ion. This is due to the occurrence of an unquenched orbital contribution typical of the  $^4T_{1g}$  ground state in six-coordinated Co(II) complexes.<sup>18</sup> As the sample is cooled from room temperature, the  $\chi_M T$  value decreases first slowly and then rapidly. The temperature dependence of the reciprocal susceptibilities ( $1/\chi_M$ ) obeys the Curie-Weiss law above 30 K with a Weiss constant  $\theta = -13.11$  K and Curie constant  $C = 3.23$   $\text{cm}^3 \cdot \text{K} \cdot \text{mol}^{-1}$  for **2** and  $\theta = -12.66$  K and  $C = 3.23$   $\text{cm}^3 \cdot \text{K} \cdot \text{mol}^{-1}$  for **3**. The magnetic behavior and the negative  $\theta$  value suggest that antiferromagnetic interactions are operative in **2** and **3**.

For complex **4**, the experimental  $\chi_M T$  value at 300 K is 1.51  $\text{cm}^3 \cdot \text{mol}^{-1} \cdot \text{K}$ , which is larger than the spin-only value (1.0  $\text{cm}^3 \cdot \text{mol}^{-1} \cdot \text{K}$ ) expected for a magnetically isolated Ni(II) ion. As the temperature is lowered, the  $\chi_M T$  value increases slightly, reaching a maximum value of 1.55  $\text{cm}^3 \cdot \text{mol}^{-1} \cdot \text{K}$  at 15 K, and then decreases rapidly. According to previous literatures, the *syn,anti* carboxylate bridges can mediate ferromagnetic couplings.<sup>19</sup> The bridging mode of the carboxylate group are generally indication of ferromagnetic interactions. The magnetic susceptibilities data in 15-300 K can be well fitted to the Curie-Weiss law with a Weiss constant  $\theta = 0.18$  K and Curie constant  $C = 1.51$   $\text{cm}^3 \cdot \text{K} \cdot \text{mol}^{-1}$  for **4**, revealing weak ferromagnetic interactions between the adjacent Ni(II) ions.

### Conclusions

Five new complexes based on isomeric tetracarboxylic acids, the 1,1':2',1''-terphenyl-4,4',4'',5'-tetracarboxylic acid and 1,1':2',1''-terphenyl-3,3',4',5'-tetracarboxylic acid, have been synthesized and characterized. Complexes **1-3** contain 1D infinite chains, and these 1D chains are further linked by hydrogen bonding to form 3D supramolecular networks. While complexes **4** and **5** show 3D mixed-connected network, respectively. The structural analysis indicate that the coordination modes of multicarboxylate ligand, N-donor ligands and different dispositions of the carboxylate groups of multicarboxylate ligands have a great influence on the structure of final products. Magnetic studies indicate that **2** and **3** show weak antiferromagnetic interactions, while **4** exhibits weak ferromagnetic interactions. The results demonstrate that such tetracarboxylic acid may be used as a versatile building block to construct novel coordination polymers with fascinating structures and properties, also, further synthesis, structures and properties studies of coordination frameworks with these tetracarboxylic acid are under way in our lab.

### Acknowledgments

This work was financially supported by the NSF of China (Nos. 21201109 and 21373122), the NSF of Hubei Provinces of China (2011CDA118).

### Notes and references

- <sup>a</sup> College of Materials & Chemical Engineering, Collaborative Innovation Center for Microgrid of New Energy of Hubei Province, China Three Gorges University, Yichang, 443002, China. Tel./Fax: +86-717-6397506; E-mail address: lidongsheng1@126.com (D.-S. Li).
- <sup>b</sup> College of Chemistry and Chemical Engineering, Luoyang Normal University, Luoyang 471022, China.
- <sup>†</sup> Electronic Supplementary Information (ESI) available: [X-ray crystallographic files in CIF format, selected bond lengths and angles for **1-5**. H-bonding geometries for **1-5**. PXRD and TGA plots of **1-4**. CCDC reference numbers: 1010213 for **1**, 1010214 for **2**, 1010215 for **3**, 958450 for **4**, and 1010216 for **5**. These data can be obtained free of charge from The Cambridge Crystallographic Data Centre via [www.ccdc.cam.ac.uk/data\\_request/cif](http://www.ccdc.cam.ac.uk/data_request/cif).] See DOI: 10.1039/c0ce000000/
- (a) H. Furukawa, K. E. Cordova, M. O'Keeffe, O. M. Yaghi, *Science*, 2013, **341**, 974; (b) J. A. Mason, M. Veenstra, J. R. Long, *Chem. Sci.*, 2014, **5**, 32; (c) M. M. Deshmukh, M. Ohba, S. Kitagawa, S. Sakaki, *J. Am. Chem. Soc.*, 2013, **135**, 4840; (d) M. H., Choi, H. J. Park, D. H. Hong, M. P. Suh, *Chem.-Eur. J.*, 2013, **19**, 17432; (e) Y.-P. He, Y.-X. Tan, J. Zhang, *Chem. Commun.*, 2013, **49**, 11323; (f) L. Kunhao, J. Y. Lee, D. H. Olson, T. J. Emge, W. Bi, M. J. Eibling, J. Li, *Chem. Commun.*, 2008, 6123; (g) H.-H. Zou, Y.-P. He, L.-C. Gui, F.-P. Liang, *CrystEngComm*, 2011, **13**, 3325; (h) D.-S. Li, Y.-P. Wu, J. Zhao, J. Zhang, J. K. Lu, *Coord. Chem. Rev.*, 2014, **261**, 1; (i) G.-P. Yang, L. Hou, X.-J. Luan, B. Wu, and Y.-Y. Wang, *Chem. Soc. Rev.*, 2012, **41**, 6992.
- (a) C. Wu, W. Lin, *Angew. Chem., Int. Ed.*, 2007, **46**, 1075; (b) S.-L. Huang, A.-Q. Jia, G.-X. Jin, *Chem. Commun.*, 2013, **49**, 2403; (c) Y. Xie, T.-T. Wang, X.-H. Liu, K. Zou, W.-Q. Deng, *Nat. Commun.*, 2013, **4**, 1960; (d) J.-R. Li, J. Sculley, H.-C. Zhou, *Chem. Rev.*, 2012, **112**, 869; (e) M. Opanasenko, M. Shamzhy, M. Lamac, J. Cejka, *Catal. Today*, 2013, **204**, 94; (f) M. Pintado-Sierra, A. M. Rasero-Almansa, A. Corma, M. Iglesias, F. Sanchez, *J. Catal.*, 2013, **299**, 137; (g) D.-S. Li, P. Zhang, J. Zhao, Z.-F. Fang, M. Du, K. Zou, Y.-Q. Mu, *Cryst. Growth Des.*, 2012, **12**, 1697; (h) G.-P. Yang, L. Hou, L.-F. Ma, and Y.-Y. Wang, *CrystEngComm*, 2013, **15**, 2561.
- (a) Z. Chen, X. Wu, S. Qin, C. Lei, F. Liang, *CrystEngComm*, 2011, **13**, 2029; (b) M. Kurmoo, *Chem. Soc. Rev.*, 2009, **38**, 1353; (c) Y.-P. Wu, D.-S. Li, F. Fu, W.-W. Dong, J. Zhao, K. Zou, Y.-Y. Wang, *Cryst. Growth Des.*, 2011, **11**, 3850; (d) M.-H. Zeng, Y.-L. Zhou, M.-C. Wu, H.-L. Sun, M. Du, *Inorg. Chem.*, 2010, **49**, 6436; (e) J. Cui, Y. Li, Z. Guo, H. Zheng, *Chem. Commun.*, 2013, **49**, 555; (f) S.-D. Han, J.-P. Zhao, Y.-Q. Chen, S.-J. Liu, X.-H. Miao, T.-L. Hu, X. H. Bu, *Cryst. Growth Des.*, 2014, **14**, 2; (g) L. Hou, Y.-Y. Lin, X.-M. Chen, *Inorg. Chem.*, 2008, **47**, 1346.
- (a) X. Zhu, Q. Chen, Z. Yang, B.-L. Li, H.-Y. Li, *CrystEngComm.*, 2013, **15**, 471; (b) X.-M. Zhang, M.-L. Tong, X.-M. Chen, *Angew. Chem., Int. Ed.*, 2002, **41**, 1029; (c) T. Ohmura, W. Mori, M. Hasegawa, T. Takei, A. Yoshizawa, *Chem. Lett.*, 2003, **32**, 34; (d) L. Hou, Y.-Y. Lin, X.-M. Chen, *Inorg. Chem.*, 2008, **47**, 134; (e) W. G. Lu, C. Y. Su, T. B. Lu, L. Jiang, J. M. Chen, *J. Am. Chem. Soc.*, 2006, **128**, 34; (f) D.-S. Li, J. Zhao, Y.-P. Wu, B. Liu, L. Bai, Z. Kun, M. Du, *Inorg. Chem.*, 2013, **51**, 8091.
- (a) S. K. Ghosh, R. Joan and P. K. Bharadwaj, *Cryst. Growth Des.*, 2005, **5**, 623. (b) X. Zhou, H. Li, H. Xiao, L. Li, Q. Zhao, T. Yang, J. Zuo, W. Huang, *Dalton Trans.*, 2013, **42**, 5718; (c) Y. Zhao, D.-S. Deng, L.-F. Ma, B.-M. Ji, L.-Y. Wang, *Chem. Commun.*, 2013, **49**, 10299; (d) K. Sumida, D. L. Rogow, J. A. Mason, T. M. McDonald, E. D. Bloch, Z. R. Herm, T.-H. Bae, J. R. Long, *Chem. Rev.*, 2012, **112**, 724; (e) J. Q. Liu, B. Liu, Y. Y. Wang, P. Liu, G. P. Yang, R. T. Liu, Q. Z. Shi, S. R. Batten, *Inorg. Chem.*, 2010, **49**, 10422; (f) P. Horcajada, R. Gref, T. Baati, P. K. Allan, G. Maurin, P. Couvreur, G. Férey, R. E. Morris, C. Serre, *Chem. Rev.*, 2012, **112**, 1232; (g) S. M. Fang, E. C. Sanudo, M. Hu, Q. Zhang, S. T. Ma, L. R. Jia, C. Wang, J. Y. Tang, M. Du, C. S. Liu, *Cryst. Growth Des.*, 2011, **11**, 811.
- (a) F.-P. Huang, H.-Y. Li, H.-D. Bian, J.-L. Tian, S.-P. Yan, D.-Z. Liao, P. Cheng, *CrystEngComm.*, 2012, **14**, 4756; (b) X. Wang, Y. Liu, C. Xu, Q. Guo, H. Hou, Y. Fan, *Cryst. Growth Des.*, 2012, **12**, 2435; (c) J.-H. He, D.-Z. Sun, D.-R. Xiao, S.-W. Yan, H.-Y. Chen, J. Yang, E.-



- B. Wang, *Polyhedron*, 2012, **42**, 24; (d) G.-H. Cui, C.-H. He, C.-H. Jiao, J.-C. Geng, V. A. Blatov, *CrystEngComm*, 2012, **14**, 4210; (e) F.-J. Liu, H.-J. Hao, C.-J. Sun, X.-H. Lin, H.-P. Chen, R.-B. Huang, L.-S. Zheng, *Cryst. Growth Des.*, 2012, **12**, 2004; (f) D. Sun, R. Cao, Y. Liang, Q. Shi, M. Hong, *J. Chem. Soc., Dalton Trans.*, **2002**, 1847; (g) X. Li, Y. Wang, Z. Ma, R. Zhang, J. Zhao, *J. Coord. Chem.*, 2010, **63**, 1029; (h) J.-D. Lin, J.-W. Cheng, S.-W. Du, *Cryst. Growth Des.*, 2008, **8**, 3345; (i) Y. Feng, E.-C. Yang, M. Fu, X.-J. Zhao, *Z. Anorg. Allg. Chem.*, 2010, **636**, 253.
- 7 (a) M.-T. Ding, J.-Y. Wu, Y.-H. Liu, J.-L. Lu, *Inorg. Chem.*, 2009, **48**, 7457; (b) C. Volkringer, T. Loiseau, M. Haoua, F. Taulelle, D. Popov, M. Burghammer, C. Riekel, C. Zlotea, F. Cuevas, M. Latroche, D. Phanon, C. Knöfelv, P. L. Llewellyn, G. Férey, *Chem. Mater.*, 2009, **21**, 5783; (c) H.-Y. Bai, J.-F. Ma, J. Yang, L.-P. Zhang, J.-C. Ma, Y.-Y. Liu, *Cryst. Growth Des.*, 2010, **10**, 1946; (d) A. M. Kirillov, Y. Y. Karabach, M. V. Kirillova, M. Haukka, A. J. L. Pombeiro, *Cryst. Growth Des.*, 2012, **12**, 1069; (e) L. Wen, J. Zhao, K. Lv, K. Deng, X. Leng, D. Li, *Cryst. Growth Des.*, 2012, **12**, 1603; (f) S. R. Caskey, A. J. Matzger, *Inorg. Chem.*, 2008, **47**, 7942; (g) L.-M. Zhao, B. Zhai, D.-L. Gao, W. Shi, B. Zhao, P. Cheng, *Inorg. Chem. Commun.*, 2010, **13**, 1014; (h) E.-C. Yang, Y. Feng, Z.-Y. Liu, T.-Y. Liu, X.-J. Zhao, *CrystEngComm*, 2011, **13**, 230; (i) S.-H. Huang, S.-L. Wang, *Angew. Chem., Int. Ed.*, 2011, **50**, 5319.
- 8 (a) L.-Y. Pang, P. Liu, C.-P. Zhang, X. Chen, B. Chen, Y.-Y. Wang, Q.-Z. Shi, *Inorg. Chim. Acta*, 2013, **403**, 43; (b) W. Meng, Z. Xu, J. Ding, D. Wu, X. Han, H. Hou, Y. Fan, *Cryst. Growth Des.*, 2014, **14**, 730.
- 9 J. Cao, Y. Gao, Y. Wang, C. Du, Z. Liu, *Chem. Commun.*, 2013, **49**, 6897.
- 10 (a) S. Zhou, Y.-G. Chen, B. Liu, X.-M. Li, D.-X. Wang, *Eur. J. Inorg. Chem.*, **2013**, 6097; (b) Y.-L. Wei, X.-Y. Li, T.-T. Kang, S.-N. Wang, S.-Q. Zang, *CrystEngComm*, 2014, **16**, 223; (c) J.-Q. Liu, J. Wu, Y.-Y. Wang, D.-Y. Ma, *J. Coord. Chem.*, 2012, **65**, 1303; (d) L.-F. Ma, L.-Y. Wang, Y.-Y. Wang, M. Du, J.-G. Wang, *CrystEngComm*, 2009, **11**, 109; (e) J. Guo, D. Sun, L. Zhang, Q. Yang, X. Zhao, D. Sun, *Cryst. Growth Des.*, 2012, **12**, 5649; (f) F.-Y. Yi, S. Dang, W. Yang, Z.-M. Sun, *CrystEngComm*, 2013, **15**, 8320.
- 11 (a) B. F. Hoskins, R. Robson, D. A. Slizys, *J. Am. Chem. Soc.*, 1997, **119**, 2952; (b) J. Fan, C. Slebodnick, R. Angel and B. E. Hanson, *Inorg. Chem.*, 2005, **44**, 552; (c) E.-Q. Gao, Y.-X. Xu, C.-H. Yan, *CrystEngComm*, 2004, **6**, 298; (d) L.-L. Wen, Y.-Z. Li, Z.-D. Lu, J.-G. Lin, C.-Y. Duan, Q.-J. Meng, *Cryst. Growth Des.*, 2006, **6**, 530; (e) P. C. M. Dacan, D. M. L. Goodgame, S. Menzer, D. J. Williams, *Chem. Commun.*, **1996**, 2127; (f) X. Li, R. Cao, W. Bi, Y. Wang, Y. Wang, X. Li, Z. Guo, *Cryst. Growth Des.*, 2005, **5**, 1651.
- 12 (a) J. Cui, Y. Li, Z. Guo, H. Zheng, *Cryst. Growth Des.*, 2012, **12**, 3610; (b) M.-L. Han, S.-H. Li, L.-F. Ma, L.-Y. Wang, *Inorg. Chem. Commun.*, 2012, **20**, 340; (c) X.-L. Sun, Z.-J. Wang, S.-Q. Zang, W.-C. Song, C.-X. Du, *Cryst. Growth Des.*, 2012, **12**, 4431; (d) X. He, X.-P. Lu, Z.-F. Ju, C.-J. Li, Q.-K. Zhang, M.-X. Li, *CrystEngComm*, 2013, **15**, 2731; (e) G.-Z. Liu, X.-D. Li, X.-L. Li, L.-Y. Wang, *CrystEngComm*, 2013, **15**, 2428; (f) Y.-N. Zhang, Z. Dong, X. Hai, L. Cui, Y.-Y. Wang, *J. Coord. Chem.*, 2013, **66**, 1676.
- 14 (a) Y.-Q. Lan, S.-L. Li, X.-L. Wang, K.-Z. Shao, D.-Y. Du, Z.-M. Su, E.-B. Wang, *Chem.-Eur. J.*, 2008, **14**, 9999; (b) C.-J. Zhang, H.-J. Pang, Q. Tang, H.-Y. Wang, Y.-G. Chen, *J. Solid State Chem.*, 2010, **183**, 2945; (c) X.-L. Wang, J.-Li, A.-X. Tian, D. Zhao, G.-C. Liu, H.-Y. Lin, *Cryst. Growth Des.*, 2011, **11**, 3456; (d) J.-Q. Liu, Y.-Y. Wang, T. Wu, J. Wu, *CrystEngComm*, 2012, **14**, 2906; (e) J.-B. Li, X. Y. Dong, L.-H. Cao, S.-Q. Zang, T. C. W. Mak, *CrystEngComm*, 2012, **14**, 4444; (f) X.-H. Chang, L.-F. Ma, H. Guo, L.-Y. Wang, *Cryst. Growth Des.*, 2012, **12**, 3638.
- 15 Rigaku (2011). *CrystalClear*. Rigaku Americas, The Woodlands, Texas, USA, and Rigaku Corporation, Tokyo, Japan.
- 16 G. M. Sheldrick, *Acta Crystallogr.*, 2008, **A64**, 112.
- 17 (a) Q. Chu, Z. Su, J. Fan, T. Okamura, G.-C. Lv, G. X. Liu, W.-Y. Sun, N. Ueyama, *Cryst. Growth Des.*, 2011, **11**, 3885; (b) J. Ni, K.-J. Wei, Y. Liu, X.-C. Huang, D. Li, *Cryst. Growth Des.*, 2010, **10**, 3964; (c) G.-C. Ou, X.-L. Feng, T.-B. Lu, *Cryst. Growth Des.*, 2011, **11**, 851; (d) A. Stephenson, S. P. Argent, T. Riis-Johannessen, I. S. Tidmarsh, M. D. Ward, *J. Am. Chem. Soc.*, 2011, **133**, 858; (e) M.-L. Han, J.-G. Wang, L.-F. Ma, H. Guo, L.-Y. Wang, *CrystEngComm*, 2014, **14**, 2691.
- 18 (a) R.L. Carlin, *Magnetochemistry*; Springer-Verlag: Berlin, Heidelberg, **1986**; (b) F. E. Mabbs, D. J. Machin, *Magnetism and Transition Metal Complexes*; Chapman and Hall Ltd.: London, **1973**.
- 19 (a) L.-F. Ma, M.-L. Han, J.-H. Qin, L.-Y. Wang, and M. Du, *Inorg. Chem.*, 2012, **51**, 9431; (b) D. Ghoshal, G. Mostafa, T. K. Maji, E. Zangrando, T. H. Lu, J. Ribas, and N. R. Chaudhuri, *New J. Chem.*, 2004, **28**, 1204.

**Graphical Abstract:**

**Title:** A series of divalent metal coordination polymers based on isomeric tetracarboxylic acid: Syntheses, structures and magnetic properties

**Key Topic:**

A series of M(II) coordination polymers have been synthesized under hydrothermal conditions. Complex **1-3** contain 1D infinite chains, and these 1D chains are further linked by hydrogen bonding to form 3D supramolecular networks. While complexes **4** and **5** show tetra- or penta-nodal 3D network, respectively.

